

**Dynamical instability of electric-field domains in ac-driven superlattices**Rosa López,<sup>1,2</sup> David Sánchez,<sup>1,2</sup> and Gloria Platero<sup>1</sup><sup>1</sup>*Instituto de Ciencia de Materiales de Madrid (CSIC), Cantoblanco, 28049 Madrid, Spain*<sup>2</sup>*Département de Physique Théorique, Université de Genève, CH-1211 Genève, Switzerland*

(Received 11 November 2002; published 31 January 2003)

We analyze theoretically the dynamical transport through a weakly coupled semiconductor superlattice, under an ac potential with frequencies in the THz regime, by means of a general model for time-dependent sequential tunneling within a nonequilibrium-Green's-function framework. Highly doped superlattices present, under certain conditions, the formation of electric-field domains at a static dc voltage bias. We find that the THz signal drives the system from a stationary current toward an oscillatory time dependence as the ac intensity increases. However, the current oscillates periodically in the MHz regime, reflecting an ac-induced motion and recycling of traveling domain walls. Finally, we predict that on further increasing the intensity of the ac potential, the tunneling current undergoes a transition from a periodically time-dependent state to a stationary one in which a homogeneous electric-field distribution builds up along the sample.

DOI: 10.1103/PhysRevB.67.035330

PACS number(s): 73.21.Cd, 73.40.Gk, 73.50.Fq

**I. INTRODUCTION**

The peculiar synergy between ac forcing potentials and quantum confinement has given rise to phenomena observed in double barriers, double quantum wells (QW's), and superlattices (SL's).<sup>1-9</sup> As a brief survey, we should mention negative pumping of electrons,<sup>10,11</sup> dynamical localization,<sup>11,12</sup> photoinduced sequential tunneling,<sup>13</sup> bistability between positive and negative current,<sup>14</sup> and recently proposed Fermi pumps.<sup>15</sup> In addition, the effect of an ac potential in strongly interacting nanostructures such as quantum wires,<sup>16</sup> quantum dots, and double quantum dots has been addressed recently.<sup>17-20</sup> However, the majority of the experimental and theoretical works have dealt with *stationary* transport properties and the *dynamical* behavior of driven nanostructures has been comparatively neglected. An attempt in this direction is given in this work.

Weakly coupled *n*-doped semiconductor SL's have been shown to exhibit a rich variety of strongly nonlinear behavior resulting from the interplay between resonant tunneling processes and charging effects.<sup>21</sup> In the high-doping case, this is reflected in the formation of electric-field domains inside the SL when an external dc bias is applied in the contact regions. More exciting is the spontaneous generation of self-sustained oscillations of the electric current at a fixed dc bias when the well doping is lowered. Recently, experimental<sup>22</sup> and theoretical<sup>23</sup> studies have addressed the influence of a low-frequency ac signal on the time-dependent current in SL's. The application of an external ac potential, though very weak, has been shown to dramatically alter the dynamical state of the system. When the ac frequency is incommensurate with the natural frequency of the SL, intriguing routes to chaos giving rise to complicated Poincaré maps have been observed.<sup>24</sup> In that case, the ac frequency is of the order of tens of MHz and it results in an adiabatic modulation of the SL electrostatic drops.

Here, we are interested in the opposite regime—we investigate the time dependent current through a multiple-quantum-well system driven by a *high*-frequency ac potential,  $V_i^{\text{ac}}(t) = V_i^{\text{ac}} \cos(\omega_0 t)$ , where  $f_{\text{ac}} = \omega_0/2\pi$  is of the order of

several THz, and  $V_i^{\text{ac}}$  is the ac amplitude in the *i*th well. It is well known that in this case photoassisted tunneling takes place, and the electronic states develop sidebands which act as new tunneling channels.<sup>5,14</sup> Furthermore, as the applied ac frequency and intensity are of the order of the typical energies in a semiconductor QW (energy levels and broadening due to scattering of the order of tens of meV), they should be incorporated on equal footing. The competition between these scales of energy is thus expected to give rise to different properties. In Ref. 14, the time-averaged transmission probability for electrons tunneling sequentially in the presence of an ac potential was studied by means of a transfer-Hamiltonian-based model. Local equilibrium within the QW's was assumed in order to calculate the *stationary* current. In this work, our aim is to present a model for studying the *dynamics* of the sequential current in ac-driven weakly coupled SL's in the THz regime. The application of a time-dependent potential to a nanostructure breaks the time-translational invariance of the system. To fully address this nonequilibrium situation, we use the Keldysh formalism which allows us to obtain general expressions for the tunneling current in the presence of an ac potential. The electron-electron interaction will be included self-consistently within a mean-field (Hartree) approximation along with appropriate boundary conditions.<sup>25,26</sup>

The paper is organized as follows. In Sec. II, we thoroughly explain the theoretical model that we use to calculate the sequential-tunneling current through a dc-biased multiple-quantum-well structure in the presence of an intense ac potential. Section III contains our numerical results and we discuss the ac-induced dynamical transition that we find. Eventually, in Sec. IV we present the conclusions.

**II. THEORETICAL MODEL**

The Hamiltonian for independent electrons in weakly coupled *N* QW's under the influence of an ac potential is given by

$$\begin{aligned}
\mathcal{H} = & \sum_{k_i, i \in \{L, R\}} [E_{k_i} + V_i^{\text{ac}} \cos(\omega_0 t)] c_{k_i}^\dagger c_{k_i} \\
& + \sum_{i=1}^N \sum_{k_i} [E_{k_i} + V_i^{\text{ac}} \cos(\omega_0 t)] d_{k_i}^\dagger d_{k_i} \\
& + \sum_{\substack{k_i k_j \\ i=L \\ i=R}}^{i=L, j=1} (T_{k_i k_j} c_{k_i}^\dagger d_{k_j} + \text{H.c.}) \\
& + \sum_{i=1}^{N-1} \sum_{k_i k_{i+1}} (T_{k_i k_{i+1}} d_{k_i}^\dagger d_{k_{i+1}} + \text{H.c.}). \quad (1)
\end{aligned}$$

Here,  $c_{k_i}^\dagger (c_{k_i})$  are the creation (annihilation) operators in the leads,  $d_{k_i}^\dagger (d_{k_i})$  are the creation (annihilation) operators in the wells, and  $T_{k_i k_j}$  are the tunneling matrix elements.  $k_i$  represents the set of the quantum numbers. We will assume that the quasiparticle spectrum in the QW's will be that of an isolated two-dimensional electron gas:  $E_{k_i} = \hbar^2 k_{i,\parallel}^2 / 2m + k_{i,z}$ . Here,  $m$  is the effective mass and  $z$  is the direction perpendicular to the interfaces. Finally, in Eq. (1), the emitter (collector) lead is denoted by  $L$  ( $R$ ).

The tunneling current traversing the  $i$ th QW is derived from the time evolution of the particle density  $n_i$ :<sup>27</sup>

$$\langle \dot{n}_i \rangle = \frac{i}{\hbar} \langle [n_i, \mathcal{H}] \rangle, \quad (2)$$

where  $n_i = \sum_{k_i} d_{k_i}^\dagger d_{k_i}$ . Now we made use of the continuity equation which links the particle density at the  $i$ th well to the current density flowing from the  $(i-1)$ th QW to the  $i$ th QW,  $I_{i-1,i}$ , and to the current density flowing from the  $i$ th QW to the  $(i+1)$ th QW,  $I_{i,i+1}$ :

$$\langle \dot{n}_i \rangle = \frac{I_{i,i+1} - I_{i-1,i}}{e}, \quad (3)$$

where  $I_{i,i+1}$  and  $I_{i-1,i}$  take the following form:

$$\begin{aligned}
I_{i-1,i}(t) = & -\frac{ie}{\hbar} \left[ \sum_{k_{i-1} k_i} T_{k_{i-1} k_i} \langle d_{k_{i-1}}^\dagger(t) d_{k_i}(t) \rangle \right. \\
& \left. - T_{k_i k_{i-1}}^* \langle d_{k_i}^\dagger(t) d_{k_{i-1}}(t) \rangle \right], \quad (4)
\end{aligned}$$

and

$$\begin{aligned}
I_{i,i+1}(t) = & -\frac{ie}{\hbar} \sum_{k_i k_{i+1}} [T_{k_i k_{i+1}} \langle d_{k_i}^\dagger(t) d_{k_{i+1}}(t) \rangle \\
& - T_{k_{i+1} k_i}^* \langle d_{k_{i+1}}^\dagger(t) d_{k_i}(t) \rangle]. \quad (5)
\end{aligned}$$

Equations (4) and (5) may be written in terms of the following off-diagonal nonequilibrium Green's functions:

$$G_{k_i k_j}^<(t, t') = i \langle d_{k_j}^\dagger(t') d_{k_i}(t) \rangle. \quad (6)$$

Applying the analytic continuation rules of Ref. 28 to the equation of motion of the off-diagonal time-ordered Green's

functions [Eq. (6)] along a complex contour (Keldysh, Kadanoff-Baym, etc.), one readily obtains an expression for the tunneling current flowing from the  $i$ th QW to the  $(i+1)$ th QW:

$$\begin{aligned}
I_{i,i+1}(t) = & \frac{2e}{\hbar} \text{Re} \sum_{k_i k_{i+1}} |T_{k_i k_{i+1}}|^2 \int d\tau [G_{k_{i+1}}^r(t, \tau) g_{k_i}^<(\tau, t) \\
& + G_{k_{i+1}}^<(t, \tau) g_{k_i}^a(\tau, t)], \quad (7)
\end{aligned}$$

Here,  $g_{k_i}^{a(<)}$  is the advanced (lesser) Green's function which includes the effect of the ac signal and scattering processes for an isolated QW. The scattering processes allow a non-equilibrium quasiparticle to relax its excess energy (e.g., due to interactions with ionized impurities or LO phonons). We use a phenomenological relaxation-time approximation by introducing a self-energy as an energy-independent constant (which is denoted by  $\gamma = \text{Im} \Sigma_{\text{sc}}$ ). Of course, this model might be improved by means of a microscopic calculation of  $\Sigma_{\text{sc}}$  due to the aforementioned scattering processes or even due to electronic exchange-correlation effects. In fact, exchange interaction effects have been shown to alter the absorption coefficient in QW's and SL's.<sup>29</sup> Nevertheless, we account for the Coulomb interaction in a mean-field scheme, which is a good approximation in large-area heterostructures for the physical effects discussed below. To include exchange effects would result in a loss of simplicity of the model, and we expect them not to alter qualitatively the results discussed below. Indeed,  $\Sigma_{\text{sc}}$  may vary substantially from sample to sample. In our calculations we shall take  $\gamma$  from available experimental data.<sup>10</sup>

On the other hand, in Eq. (7)  $G_{k_i}^{r(<)}$  corresponds to the retarded (lesser) Green's function which includes tunneling events. Now, our task consists of deriving the explicit formulas for these Green's functions in the sequential tunneling regime, which is the dominant mechanism in weakly coupled SL's.<sup>21</sup> In this regime, the scattering lifetime ( $\sim 1$  ps) is much shorter than the tunneling time ( $\sim 1$  ns) and thus the tunneling self-energy can be neglected to a good extent in  $G_{k_i}^{r(<)}$ . As a result, one assumes an *equilibrium* distribution function for each QW, since the electrons that tunnel relax their energy excess almost instantaneously. Taking into account these considerations, the effect of the ac potential consists of introducing a global phase in the expression for these Green's functions:  $G_{k_i}^{r(<)}(t, t') = \exp[(ieV_i^{\text{ac}}/\hbar\omega_0)(\sin\omega_0 t - \sin\omega_0 t')] \bar{G}_{k_i}^{r(<)}(t-t')$ , where  $\bar{G}_{k_i}^{r(<)}(t-t')$  is the static retarded (lesser) QW Green's function. They have the following expressions:

$$\bar{G}_{k_i}^r(t-t') = -i\theta(t-t') \exp[-i(E_{k_i} + \gamma)(t-t')], \quad (8)$$

and

$$\bar{G}_{k_i}^<(t-t') \approx \int \frac{d\epsilon}{2\pi} e^{i\epsilon(t-t')} \frac{2\gamma}{(\epsilon - E_{k_i})^2 + \gamma^2} f_i(\epsilon), \quad (9)$$

where  $f_i(\epsilon)$  is the Fermi-Dirac distribution function for the

$i$ th QW,  $f_i(\epsilon) = 1/[1 + \exp(\epsilon - \epsilon_{\omega_i})/k_B T]$  ( $\epsilon_{\omega_i}$  is the Fermi energy at the  $i$ th QW and  $T$  is taken as the lattice temperature<sup>30</sup>). A similar transformation applies for  $g_{k_i}^{a,<}(t, t')$ . Eventually, by inserting the obtained expres-

sions for the nonequilibrium Green's functions [ $G_{k_{i+1}}^{r,<}(t, t')$  and  $g_{k_i}^{a,<}(t, t')$ ] into Eq. (7), we arrive at the expression for the tunneling current between two QW's irradiated with a THz field in the sequential tunneling regime:

$$I_{i,i+1}(t) = \frac{2e}{\hbar} \sum_{k_i, k_{i+1}} |T_{k_i, k_{i+1}}|^2 \sum_{m=-\infty}^{m=\infty} J_m(\beta) \left\{ \cos(\beta \sin \omega_0 t - m \omega_0 t) \int d\epsilon [A_{k_{i+1}}(\epsilon + m\hbar\omega_0) A_{k_i}(\epsilon) [f_i(\epsilon) - f_{i+1}(\epsilon + m\hbar\omega_0)] + \sin(\beta \sin \omega_0 t - m \omega_0 t) \int d\epsilon [A_{k_{i+1}}(\epsilon + m\hbar\omega_0) \text{Re} \bar{g}_{k_i, k_i}^a(\epsilon) f_{i+1}(\epsilon + m\hbar\omega_0) + \text{Re} \bar{G}_{k_{i+1}, k_{i+1}}^r(\epsilon + m\hbar\omega_0) A_{k_i}(\epsilon) f_i(\epsilon)] \right\}, \quad (10)$$

where  $A_{k_i}$  is the spectral function for the  $i$ th isolated QW including scattering, and  $J_p$  is the  $p$ th Bessel function whose argument is given by  $\beta = e(V_i^{\text{ac}} - V_{i+1}^{\text{ac}})/\hbar\omega_0$ . Notice that here we assume that the ac potential is spatially uniform along a QW (but different from that of its neighbors) and  $\beta$  is independent of the QW index.<sup>3</sup>

The current (10) may be written as  $I(t) = I_0 + \sum_{l>0} [I_l^{\text{cos}} \cos(l\omega_0 t) + I_l^{\text{sin}} \sin(l\omega_0 t)]$ , where  $I_0$  is the time-averaged current.  $I_l^{\text{cos}}$  and  $I_l^{\text{sin}}$  contain higher harmonics for  $l>0$ . Now, since we are interested in the photoassisted tunneling regime, we require  $\hbar\omega_0 > \gamma$ .<sup>10</sup> This means that the electrons experience at least one cycle of the ac potential between two successive scattering events. In addition, the scattering lifetime represents the lowest temporal cutoff above which our assumption of local equilibrium within each QW holds. Therefore, the *explicit* time variation of  $I(t)$  vanishes and we are left with the *implicit* change of  $I_0$  with respect to time. This variation (in time scales larger than  $\hbar/\gamma$ ) results from the evaluation of the continuity equation for  $i=1, \dots, N$ , where  $N$  is the number of wells, supplemented with Poisson equations, constitutive relations, and realistic boundary conditions.<sup>26,31</sup> In the following paragraphs, we shall elaborate on this.

The total current density traversing the sample is the sum of the tunneling current plus the displacement current, i.e.,  $\mathcal{I}(t) = I_{i,i+1} + (\epsilon/d)(dV_i/dt)$ , where  $\epsilon$  is the static permittivity,  $d$  is the barrier width, and  $V_i$  is the voltage drop in the  $i$ th barrier.  $I_{i,i+1}$  depends on  $n_i$  and  $n_{i+1}$ . Since we have assumed that the electrons reach local equilibrium within each QW, the electronic densities  $n_i$  depend on the QW Fermi energies  $\epsilon_{\omega_i}$ . The electronic densities are coupled to the SL electrostatic drops by means of Poisson equations. For a given set  $\{\epsilon_{\omega_i}\}$ ,  $n_i$  evolves according to the continuity equation (3). In these equations, the current (10) is a functional of the Fermi energies and the set of SL voltage drops (denoted by  $\Phi$ ):  $I_{i,i+1} = I_{i,i+1}(\epsilon_{\omega_i}, \epsilon_{\omega_{i+1}}, \Phi)$ , where  $\Phi$  is calculated with the help of discrete Poisson equations. The Poisson equation yields the potential drops in the barriers,  $V_i$  ( $i=1, \dots, N+1$ ), and in the wells,  $V_{\omega_i}$  ( $i=1, \dots, N$ ):

$$\frac{V_{\omega_i}}{w} = \frac{V_i}{d} + \frac{en_i(\epsilon_{\omega_i}) - eN_w}{2\epsilon}, \quad (11)$$

$$\frac{V_{i+1}}{d} = \frac{V_i}{d} + \frac{en_i(\epsilon_{\omega_i}) - eN_w}{\epsilon}, \quad (12)$$

where  $w$  is the well thickness, and  $N_w$  is the external doping at the QW's.

The boundary conditions at the contacts describe the lengths of the depletion and accumulation layers as well as the charge density at the leads (see Refs. 25 and 26 for a detailed discussion of the electrostatic model at the lead regions). The resulting system of algebraic-differential equations is closed after imposing charge and total voltage conservation. Notice that this system can be solved *only* self-consistently, as the transmissions  $T_{k_i, k_{i+1}}$  in Eq. (10) depend implicitly on the local electrostatic distribution through the positions of the resonant levels. In turn, the resulting  $\{\epsilon_{\omega_i}\}$  depend as well self-consistently on the voltage drops through Eqs. (11) and (12). The numerical simulation begins with physically sensible initial conditions. Then, we integrate the resulting algebraic-differential system of equations by means of backward differentiation formulas methods. The whole procedure is repeated until numerical convergence is achieved *at each time step* of Eq. (3) for  $i=1, \dots, N$ . This way, the dynamics of the total sequential current  $\mathcal{I}(t)$  is fully taken into account.

### III. RESULTS

We present results for a  $N=50$  SL with 13.3-nm GaAs wells and 2.7-nm AlAs barriers. Well doping is  $N_w = 2 \times 10^{-10} \text{ cm}^{-2}$  and we take  $\gamma = 7 \text{ meV}$  and  $f_{\text{ac}} = 3 \text{ THz}$ . In Fig. 1(a), the time average of  $\mathcal{I}(t)$  is plotted as a function of the applied dc bias,  $V$ . Without ac, the  $\mathcal{I}$ - $V$  curve shows branches after the first peak. This feature is characteristic of static electric-field domain formation.<sup>26</sup> Resonant tunneling takes place between the lowest QW subbands in part of the SL (the low-field region), whereas electrons tunnel from the

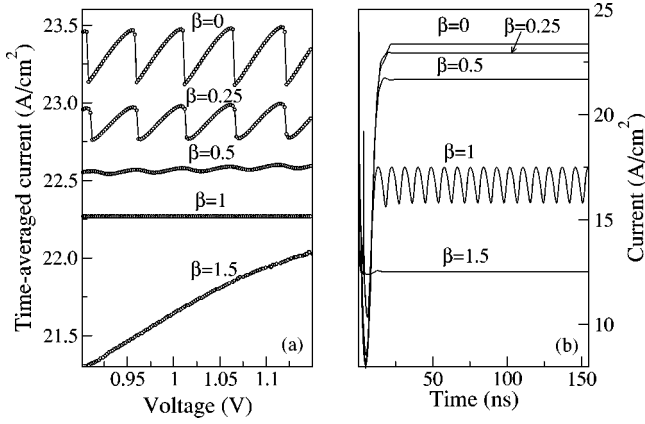


FIG. 1. (a)  $I$ - $V$  curves for different values of  $\beta$  at fixed  $f_{ac} = 3$  THz. Lines are used to guide the eye. Curves for  $\beta=0$ ,  $\beta=0.5$ ,  $\beta=1$ , and  $\beta=1.5$  have been shifted 0.05, 0.91, 5.46, and 9.35 A/cm<sup>2</sup>, respectively, for clarity. At  $\beta=0$  and  $\beta=0.25$  the electric-field domain formation is stable, the total current is stationary, and it results in discontinuous branches. With increasing  $\beta$ , branches coalesce, causing the development of an oscillatory pattern at  $\beta=0.5$ , followed by a flat plateau that is formed at  $\beta=1$ . Larger values of  $\beta$  involve a smooth, increasing curve of current with voltage (see  $\beta=1.5$ ). (b) Time-resolved electric current for a dc bias  $V=1.1$  V. The variation with  $\beta$  shows the dependence of the state character (static or dynamic) on the ac potential. Schematically, the transition (static electric-field domains)  $\rightarrow$  (moving electric-field domains) takes place at around  $\beta=1$ , whereas the process (moving electric-field domains)  $\rightarrow$  (homogeneous electric field) occurs at around  $\beta=1.5$ .

ground state to the first excited state of the downstream QW in the high-field region. In the presence of an ac signal, the branches become smoother ( $\beta=0.25$ ), and finally they coalesce and a plateau clearly forms ( $\beta=1$ ). This is the key signature of current self-oscillations. It is well known that by decreasing the doping in a SL, the electric-field domain configuration becomes unstable, and self-sustained current oscillations occur due to the periodic recycling of the domain wall.<sup>21</sup> By increasing  $\beta$  further, the plateau starts to be replaced by a positive differential resistance region. There is a similar well-known phenomenon in weakly coupled SLs driven only by dc voltages: under a critical value of the carrier density, neither static nor moving domain walls exist and the electric field drops homogeneously across the *whole* sample. This may be effectively achieved by either applying a transverse magnetic field<sup>32</sup> or raising the temperature.<sup>33</sup> In our case, the doping density is constant and it is the ac potential that tunes this transition. To illustrate this, we have calculated  $I(t)$  for a fixed bias  $V=1.1$  V [see Fig. 1(b)]. For  $\beta=0$ , the current achieves a constant value after a transient time. As  $\beta$  increases ( $\beta=1$ ), the current oscillates with a frequency in the range of MHz, much smaller than  $f_{ac}$ . This is a result of the motion of the accumulating layer of electrons, and its recycling in the highly doped contacts (see below). Then the ac potential induces a transition from a stationary configuration toward a dynamic state likely via a supercritical Hopf bifurcation. Below, we shall show that the existence of photosidebands and their influence on the non-

linear behavior of the system drives the SL toward oscillations. For  $\beta=1.5$  the current is damped and  $I(t)$  reaches a uniform value. This is a striking feature—an *oscillation disappearance induced by an ac potential*.<sup>34</sup>

The ac-induced transition from static electric-field domains toward homogeneous field distribution through self-sustained current oscillations is illustrated in Fig. 2. We observe how the charge density through the structure, at fixed dc bias, undergoes a transition from being accumulated in the 43rd QW, independently of time (stationary electric-field domains) at zero ac potential, to presenting periodic oscillations ( $\beta=1$ ). Increasing  $\beta$  further ( $\beta=1.5$ ), a homogeneous charge distribution is reached and the electric field and charge are uniformly distributed through the sample (with small inhomogeneities at the emitter contact). A qualitative explanation of this transition is as follows.

Let  $v(F)$  denote the average drift velocity due to tunneling between two QW's with local electric field  $F$ . Within a semiclassical approximation, the current (10) can be approximated by  $I_{i,i+1} = en_i v(F_i)/\mathcal{L}$ , where the electronic drift velocity is given by  $v(F) = I(N_w, N_w, F)\mathcal{L}/eN_w$ . Here, the current  $I(N_w, N_w, F)$  is evaluated by using Eq. (10) after imposing  $n_i = n_{i+1} = N_w$  and setting an average interwell electric field  $F$  along the SL period  $\mathcal{L} = d + w$ .<sup>31</sup> In what follows, we neglect the contribution from diffusivity, which can be important at very low electric fields.<sup>31</sup> As shown in Ref. 35, the sufficient condition for stationary electric-field domains to form reads

$$N_w \gtrsim N_w^{\text{eff}} \equiv \varepsilon v_m \frac{F_m - F_M}{e(v_M - v_m)}, \quad (13)$$

where  $v_M$  ( $v_m$ ) is the maximum (minimum) electron drift velocity attained at an electric field given by  $F_M$  ( $F_m$ ). Unlike the minimum velocity, the maximum drift velocity is very sensitive to the external ac potential. We see from the time average of Eq. (10) that first current peak (i.e.,  $v_M$ ) is weighted by  $J_0^2(\beta)$  at low values of  $\beta$  (the zero-photon peak). As  $\beta$  increases, the THz potential produces photoassisted tunneling with absorption and emission of photons. As a result, the zero-photon peak is quenched as the contribution of terms with  $J_{p \neq 0}^2(\beta)$  begins to grow. This is a consequence of the photoassisted formation of sidebands.<sup>10,14</sup> The overall effect is that  $N_w^{\text{eff}}$  decreases as  $\beta$  increases. For a certain critical value of  $\beta$  [ $\beta_{\text{crit}} \sim 1$ ; see Fig. 1(b)], we find  $N_w \lesssim N_w^{\text{eff}}$  and the steady electric-field domain configuration is no longer stable. The system evolves spontaneously toward self-sustained current oscillations.

On the other hand, once the dynamical configuration is stable, increasing  $\beta$  will tend to drive the SL to a trivially homogeneous electric-field profile (see Fig. 2, lower panel). The reason for that is the complicated shape of the time-averaged drift velocity induced by the ac potential. The ac potential opens up new tunneling channels due to photon absorption and emission<sup>10,14</sup> and their relative weight and their contribution to  $v(F)$  depend in a nontrivial way on the ac frequency and intensity, the sample characteristics and the scattering processes involved. This can lead to a  $I$ - $V$  curve exhibiting positive differential resistance with a  $Z$  shape un-



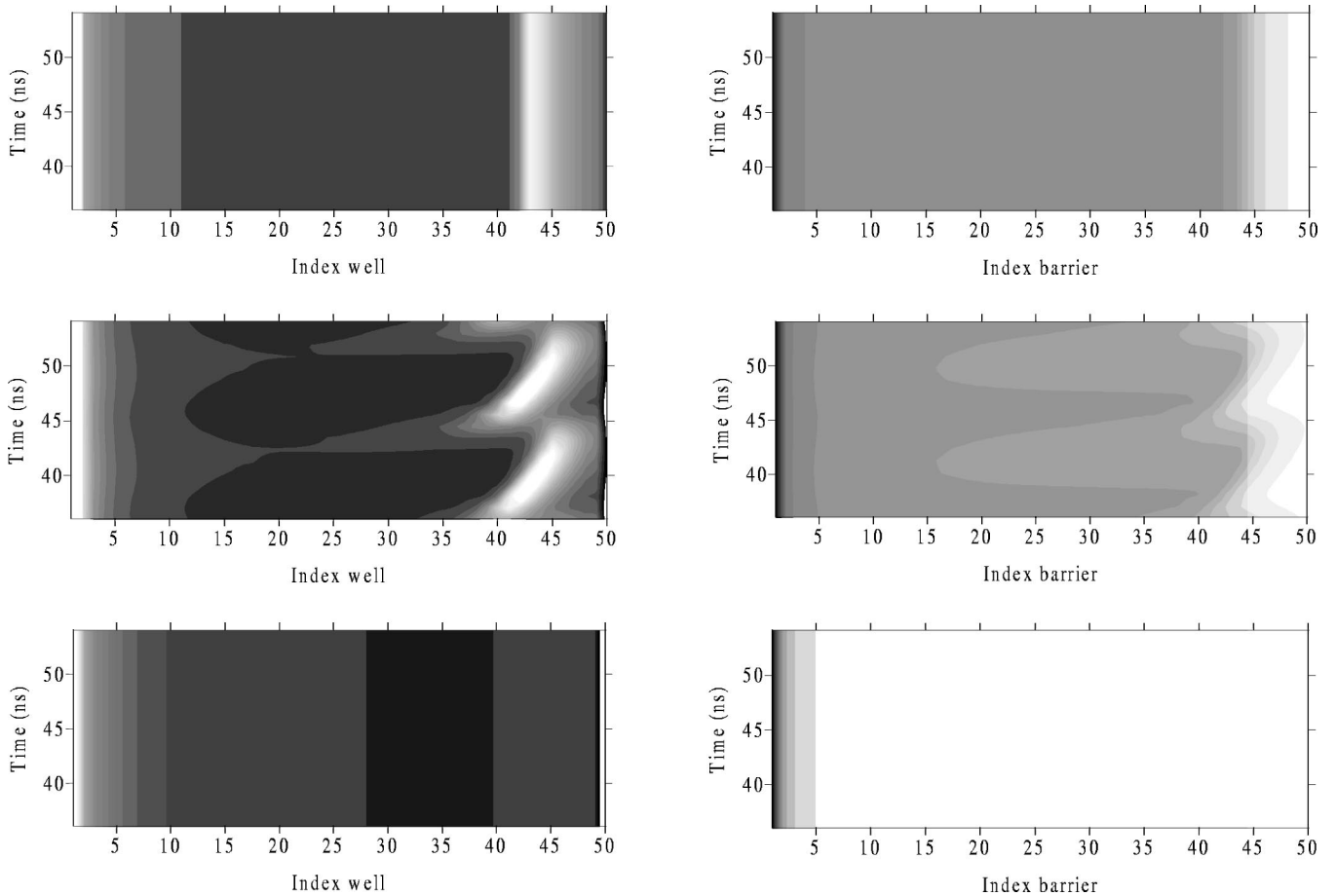


FIG. 2. Left panels: Time evolution of electron densities as a function of the index well. Lighter areas mean larger densities. Right panels: Time evolution of the voltage drop at the barriers (last barrier has been omitted for simplicity). Lighter areas indicate larger values of the electric field. Top:  $\beta=0$  (no ac potential is present). Electrons are accumulated mainly in well 43, forming a domain wall which separates high and low electric-field regions. Middle:  $\beta=1$  (self-sustained oscillations). The domain wall drifts along part of the SL. The monopole is clearly visible at well 39, moves toward well 47 and dissolves at the collector. Notice the oscillatory behavior of the electric fields, which is correlated with the monopole motion. Bottom:  $\beta=1.5$  (homogeneous case). Voltage drops almost linearly across the sample and consequently no accumulation layer is formed.

like the electric-field domain case, which exhibits a  $\mathcal{I}$ - $V$  curve with an  $N$  shape.<sup>35</sup> Even though an analytical estimation of the different transition points cannot be obtained, the previous argument explains why an ac field may induce a dynamical transition from stable stationary domains to traveling field domains and a homogeneous electrostatic configuration by modifying the effective electronic drift velocity with the dimensionless ac parameter  $\beta$ .

#### IV. CONCLUSIONS

In summary, we propose a theoretical model which allows the evaluation of the time-dependent sequential-tunneling current through dc-biased semiconductor SL's in the presence of an ac potential. We predict that an intense ac potential with a frequency of the order of the energies of the system (THz) induces a continuous transition for the current as a function of the ac intensity. The electronic current becomes time dependent with a frequency of the order of MHz. It corresponds roughly to the inverse of the tunneling rate per number of wells, as it occurs in SL's which present self-

sustained oscillations without any ac external force. By increasing the THz field intensity further, the current becomes stationary again, and the electric field is homogeneous through the sample. Hence an ac potential could be used to induce and control frequency oscillations through the sample. Notice that the role played here by the ac potential is not to serve as a special triggering, but to drive the system to a distinct dynamical state. Very recent experimental evidence in strongly coupled SL's demonstrates that the control over the internal frequencies may be feasible in the GHz regime.<sup>36</sup>

#### ACKNOWLEDGMENTS

We thank R. Aguado, L.L. Bonilla, M. Büttiker, and C. Creffield for fruitful discussions and a critical reading of the manuscript. This work was supported by the Spanish DGES Grant No. MAT2002-02465, by the European Union TMR Contract No. FMRX-CT98-0180, and by the European Community's Human Potential Program under Contract No. HPRN-CT-2000-00144, Nanoscale Dynamics.

- <sup>1</sup>M. Jonson, Phys. Rev. B **39**, 5924 (1989); P. Johansson, *ibid.* **41**, 9892 (1990); H.C. Liu, *ibid.* **43**, 12 538 (1991).
- <sup>2</sup>A.-P. Jauho, N.S. Wingreen, and Y. Meir, Phys. Rev. B **50**, 5528 (1994).
- <sup>3</sup>M. Wagner, Phys. Rev. Lett. **76**, 4010 (1996).
- <sup>4</sup>J. ĩnarrea, G. Platero, and C. Tejedor, Phys. Rev. B **50**, 4581 (1994).
- <sup>5</sup>R. Aguado, J. ĩnarrea, and G. Platero, Phys. Rev. B **53**, 10 030 (1996).
- <sup>6</sup>A.W. Ghosh, A.V. Kuznetsov, and J.W. Wilkins, Phys. Rev. Lett. **79**, 3494 (1997).
- <sup>7</sup>M.H. Pedersen and M. Büttiker, Phys. Rev. B **58**, 12 993 (1998); Ya.M. Blanter and M. Büttiker, Phys. Rep. **336**, 1 (2000).
- <sup>8</sup>N. Sashinaka, Y. Oguma, and M. Asada, Jpn. J. Appl. Phys., Part 1 **39**, 4899 (2000).
- <sup>9</sup>C. Zhang, Appl. Phys. Lett. **78**, 4187 (2001).
- <sup>10</sup>B.J. Keay, S.J. Allen, J. Galán, J.P. Kaminski, K.L. Campman, A.C. Gossard, U. Bhattacharya, and M.J.M. Rodwell, Phys. Rev. Lett. **75**, 4098 (1995).
- <sup>11</sup>G. Platero and R. Aguado, Appl. Phys. Lett. **70**, 3546 (1997).
- <sup>12</sup>F. Grossmann, T. Dittrich, P. Jung, and P. Hänggi, Phys. Rev. Lett. **67**, 516 (1991); M. Hartmann, M. Grifoni, and P. Hänggi, Europhys. Lett. **38**, 497 (1997).
- <sup>13</sup>P.S.S. Guimarães, B.J. Keay, J.P. Kaminski, and S.J. Allen, Jr., Phys. Rev. Lett. **70**, 3792 (1993).
- <sup>14</sup>R. Aguado and G. Platero, Phys. Rev. Lett. **81**, 4971 (1998).
- <sup>15</sup>M. Wagner and F. Sols, Phys. Rev. Lett. **83**, 4377 (1999).
- <sup>16</sup>M. Sasseti and B. Kramer, Phys. Rev. B **54**, R5203 (1996).
- <sup>17</sup>C. Bruder and H. Schoeller, Phys. Rev. Lett. **72**, 1076 (1994).
- <sup>18</sup>L.P. Kouwenhoven, S. Jauhar, J. Orenstein, and P.L. McEven, Phys. Rev. Lett. **73**, 3443 (1994).
- <sup>19</sup>T.H. Oosterkamp, T. Fujisawa, W. G van der Wiel, K. Ishibashi, R.V. Hijman, S. Tarucha, and L.P. Kouwenhoven, Nature (London) **395**, 873 (1998).
- <sup>20</sup>R. López, R. Aguado, G. Platero, and C. Tejedor, Phys. Rev. Lett. **81**, 4688 (1998); Phys. Rev. B **64**, 115311 (2001), and references therein.
- <sup>21</sup>L.L. Bonilla, J. Phys.: Condens. Matter **14**, R341 (2002); A. Wacker, Phys. Rep. **357**, 1 (2002).
- <sup>22</sup>K.J. Luo, H.T. Grahn, K.H. Ploog, and L.L. Bonilla, Phys. Rev. Lett. **81**, 1290 (1998).
- <sup>23</sup>O.M. Bulashenko and L.L. Bonilla, Phys. Rev. B **52**, 7849 (1995).
- <sup>24</sup>K.J. Luo, H.T. Grahn, S.W. Teitsworth, and K.H. Ploog, Phys. Rev. B **58**, 12 613 (1998); D. Sánchez, G. Platero, and L.L. Bonilla, *ibid.* **63**, 201306(R) (2001).
- <sup>25</sup>J. ĩnarrea and G. Platero, Europhys. Lett. **34**, 43 (1996).
- <sup>26</sup>R. Aguado, G. Platero, M. Moscoso, and L.L. Bonilla, Phys. Rev. B **55**, R16 053 (1997).
- <sup>27</sup>G.D. Mahan, *Many-Particle Physics*, 3rd ed. (Kluwer Academic, New York, 2000), Sec. 8.6.
- <sup>28</sup>D.C. Langreth, in *Linear and Nonlinear Electron Transport in Solids, Vol. 17 of NATO Advanced Studies Institute, Series B: Physics* edited by J.T. Devreese and V.E. Van Doren (Plenum, New York, 1976).
- <sup>29</sup>D.E. Nikonov, A. Imamoglu, L.V. Butov, and H. Schmidt, Phys. Rev. Lett. **79**, 4633 (1997); O.E. Raichev and F.T. Vasko, Phys. Rev. B **60**, 7776 (1999); A.V. Korovin, O.E. Raichev, and F.T. Vasko, *ibid.* **66**, 075306 (2002).
- <sup>30</sup>We neglect electron heating effects which could be important in the form of the local current-voltage relation of strongly coupled SL's; see H. Steuer, A. Wacker, E. Schöll, M. Ellmayer, E. Schomburg, and K.F. Renk, Appl. Phys. Lett. **76**, 2059 (2000).
- <sup>31</sup>L.L. Bonilla, G. Platero, and D. Sánchez, Phys. Rev. B **62**, 2786 (2000).
- <sup>32</sup>B. Sun, J. Wang, W. Ge, Y. Wang, D. Jiang, H. Zu, H. Wang, Y. Deng, and S. Feng, Phys. Rev. B **60**, 8866 (1999).
- <sup>33</sup>J.N. Wang, B.Q. Sun, X.R. Wang, Y. Wang, W. Ge, and H. Wang, Appl. Phys. Lett. **75**, 2620 (1999); D. Sánchez, L.L. Bonilla, and G. Platero, Phys. Rev. B **64**, 115311 (2001).
- <sup>34</sup>Notice that this effect differs qualitatively from the quenching of current self-oscillations observed by Y. Zhang, R. Klann, K.H. Ploog, and H.T. Grahn, Appl. Phys. Lett. **69**, 1116 (1996). The ac amplitude and frequency used there do not allow for the formation of sidebands and the disappearance of oscillations in favor of steady domain walls was ascribed to a locking of the domain wall motion at very high ac amplitudes when the ac frequency surpassed the inverse of the monopole dwell time.
- <sup>35</sup>A. Wacker, M. Moscoso, M. Kindelan, and L.L. Bonilla, Phys. Rev. B **55**, 2466 (1997).
- <sup>36</sup>E. Schomburg, K. Hofbeck, R. Scheuerer, M. Haeussler, K.F. Renk, A.-K. Jappsen, A. Amann, A. Wacker, D.G. Pavel'ev, and Yu. Koschurinov, Phys. Rev. B **65**, 155320 (2002).